Luminescent halido(aryl) Pt(IV) complexes obtained via oxidative addition of iodobenzene or diaryliodonium salts to bis-cyclometalated Pt(II) precursors†

Juan-Carlos López-López,[a] Delia Bautista[b] and Pablo González-Herrero*[,a]

[a]Departamento de Química Inorgánica, Facultad de Química, Universidad de Murcia, Campus de Espinardo, 19, 30100 Murcia, Spain.

[b]Área Científica y Técnica de Investigación, Universidad de Murcia, Campus de Espinardo, 21, 30100 Murcia, Spain.

†Electronic supplementary information (ESI) available: Additional experimental procedures and data, ^{1}H and $^{13}C\{^{1}H\}$ NMR spectra of new compounds, photophysical characterization, X-ray structure determinations, additional photophysical data, and computational methods and data. CCDC 2095458 (**5b**), 2095459 (**2b**), 2095460 (**5b'**·CH_2Cl_2), 2095461 (**6b**·CH_2Cl_2·H_2O) and 2095462 (**4b**·0.5CH_2Cl_2). For ESI and crystallographic data in CIF format see DOI: 10.1039/x0xx00000x

Abstract

The synthesis of bis-cyclometalated halido(aryl) Pt(IV) complexes [PtX(Ar)(C^N)$_2$], with C^N = cyclometalated 4-(*tert*-butyl)-2-phenylpyridine (bppy), 2-(*p*-tolyl)pyridine (tpy), 2-(2-thienyl)pyridine (thpy), or 1-phenylisoquinoline (piq), X = I, Cl, or F, and Ar = Ph (for all C^N ligands) or *t*-BuPh (for C^N = tpy), and the photophysical properties of the chlorido and fluorido series are reported. The oxidative addition of iodobenzene to *cis*-[Pt(C^N)$_2$] precursors is demonstrated to occur in MeCN under irradiation with visible light to give complexes [PtI(Ph)(C^N)$_2$], presumably involving radical species that also produce the activation of the solvent to give cyanomethyl complexes [PtI(CH_2CN)(C^N)$_2$]. The introduction of an aryl ligand can also be achieved by reacting *cis*-[Pt(C^N)$_2$] with (Ar_2I)PF_6 (Ar = Ph, *t*-BuPh), which affords cationic intermediates of the type [Pt(Ar)(C^N)$_2$(NCMe)]$^+$. The subsequent addition of an iodide or chloride salt gives the corresponding iodido- or chlorido(aryl) complexes. The fluorido(aryl) derivatives can be obtained from the iodido complexes by halide exchange using AgF. The chlorido- and fluorido(aryl) complexes display intense phosphorescence in deaerated CH_2Cl_2 solution and poly(methyl methacrylate) (PMMA) films at 298 K from triplet excited states primarily localized on the cyclometalated ligands (^{3}LC) with a small MLCT admixture.

Compared with the chlorido complexes, the fluorido derivatives consistently present significantly shorter emission lifetimes and higher radiative and nonradiative rate constants due to a greater MLCT contribution to the emissive state. In contrast, the introduction of the *t*-BuPh group did not induce significant changes in radiative rates with respect to the phenyl complexes.

Introduction

Complexes of late transition metal ions with heteroaromatic ligands often exhibit long-lived excited states that are accessible via photoexcitation and provide a wide applicability in light-based technologies and processes, including chemical and biological sensing,[1–3] electroluminescent materials,[4–9] photoredox catalysis,[10,11] and diverse energy-transfer processes of relevance in medicine and chemical synthesis.[12–15] Cyclometalated Pt(IV) complexes belong to a class of luminescent compounds showing ligand-centred, triplet emissive excited states (^{3}LC) with little metal character,[16,17,26,18–25] which also includes certain types of Au(III)[27–33] and Pd(II)[34,35] complexes that have been pursued as phosphors for organic light-emitting devices or photocatalysts. In previous works, we have shown that the metal contribution to the emissive excited state in cyclometalated Pt(IV) complexes with 2-arylpyridine ligands takes the form of a small but critical metal-to-ligand charge-transfer (MLCT) admixture,[16,17] which facilitates the formation of the emissive state and accelerates the radiative transition to the ground state thanks to the spin-orbit coupling effects induced by the metal. Fluctuations of the MLCT character of the emissive excited state have been observed among Pt(IV) complexes with different coordination environments, which cause variations in radiative rates and, in certain cases, in emission energies.[19,20,24] A rational way to increase this MLCT character is to destabilize the metal dπ orbitals by strengthening π donation from the ligands, which should lead to a higher metal orbital involvement in the occupied frontier orbitals. Such an effect has been observed for the fluorido complexes [$PtF_2(ppy)_2$] and [$PtF(Me)(ppy)_2$] (ppy = cyclometalated 2-phenylpyridine) with respect to the analogous chlorido complexes.[19] However, a systematic evaluation of the effects of fluoride on the luminescence of Pt(IV) complexes with different cyclometalated ligands has not been undertaken. We also note that the use of fluoride as ancillary ligand in luminescent Pt(II)[36] or Ir(III)[37] complexes is rare and the consequences of fluoride coordination on excited-state properties have not been studied in much detail.

Based on the above precedents, in the present work we have targeted bis-cyclometalated Pt(IV) complexes of the type [PtX(Ar)(C^N)$_2$], bearing two 2-arylpyridine ligands (C^N) in an unsymmetrical arrangement and mutually cis halido (X) and aryl (Ar) ligands, which could offer the possibility to modulate the MLCT admixture into the emissive state by variation of X or Ar. More specifically, we have evaluated the effects of the introduction of fluoride by comparing the emission properties of two analogous series of fluorido and chlorido complexes, and also employed two aryl ligands of different electron-donating character (Ar = Ph, *t*-BuPh) to examine their influence. Although complexes of the type [PtCl(Ar)(C^N)$_2$] have been previously reported,[21,22] all of them contain the C_6F_5 group as the aryl ligand and variations of the halide have not been investigated.

To synthesize our target derivatives, we envisaged the use of bis-cyclometalated Pt(II) complexes, *cis*-[Pt(C^N)$_2$], as precursors, which can be conveniently prepared by photochemical methods.[38,39] The introduction of the aryl ligand would then be attempted through the oxidative addition of aryl halides or diaryliodonium salts. Although oxidative addition reactions of alkyl halides to *cis*-[Pt(C^N)$_2$] complexes [C^N = cyclometalated 2-phenylpyridine or 2-(2-thienyl)pyridine] were reported by von Zelewsky and co-workers to proceed without difficulty under thermal or photochemical conditions,[40–42] aryl halides were found unreactive.[42] In fact, the intermolecular oxidative addition of aryl halides to Pt(II) complexes is extremely rare and only very recently has it been unambiguously demonstrated by Love and coworkers,[43] who showed that electron-rich complexes of the type [PtMe(C*^C)(L)] (C*^C = cyclometalated 1,3-dimesitylimidazol-2-ylidene; L = SMe_2 or pyridine) reacted with iodobenzene or bromobenzene at 60 °C to give halido(phenyl) Pt(IV) intermediates that undergo the reductive elimination of toluene. However, the isolation of an oxidative addition product was only possible by employing 2-(2-iodophenyl)pyridine, which led to a stable six-coordinate Pt(IV) complex with cyclometalated 2-phenylpyridine. Here we demonstrate that intermolecular oxidative addition of iodobenzene to *cis*-[Pt(C^N)$_2$] complexes is possible under irradiation with visible light at room temperature, providing access to stable bis-cyclometalated iodido(aryl) Pt(IV) complexes that can be transformed into the fluorido analogues via halide exchange. Alternatively, the introduction of the aryl ligand can also be achieved using diaryl iodonium salts, allowing the synthesis of chlorido(aryl) Pt(IV) complexes upon addition of a chloride salt.

Results and discussion

Synthesis

For the synthesis of the target bis-cyclometalated halido(aryl) Pt(IV) complexes, we initially attempted the oxidative addition of iodobenzene to *cis*-[Pt(C^N)$_2$] (**1a-d**), with C^N = cyclometalated 4-(*tert*-butyl)-2-phenylpyridine (bppy, **a**), 2-(*p*-tolyl)pyridine (tpy, **b**), 2-(2-thienyl)pyridine (thpy, **e**), or 1-phenylisoquinoline (piq, **d**) under irradiation with visible light (λ = 454 nm) in MeCN at room temperature. These reactions afforded mixtures containing the desired phenyl complexes [PtI(Ph)(C^N)$_2$] (**2a-d**) together with the unexpected cyanomethyl derivatives [PtI(CH$_2$CN)(C^N)$_2$] (**3a-d**) after 4 h (Scheme 1). The molar proportions of these products in the crude reaction mixtures range from 80:20 (**2a:3a**) to 40:60 (**2d:3d**), as estimated from ^{1}H NMR spectra. Complexes **2a-d** could be separated from these mixtures by column chromatography or fractional precipitation and isolated in low to moderate yields (30-47%). The purification of the cyanomethyl complexes by chromatography was not successful, except for the tpy complex **3b**, which could be isolated in 15% yield.

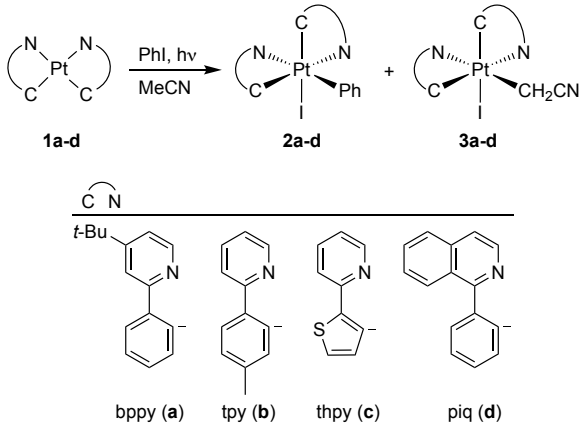

Scheme 1. Photoinitiated reactions of complexes **1a-d** with PhI.

Since these reactions did not take place in the dark, it is clear that they are photoinitiated. Based on previously described mechanisms for photochemically initiated oxidative additions of alkyl halides to Pt(II) complexes,[41,42,44] we propose the radical mechanism outlined in Scheme 2 for the formation of complexes **2** and **3**. The photoexcited precursor **1** would reduce iodobenzene producing a phenyl radical and an intermediate Pt(III) iodido complex, that would couple with each other to give **2**. In a competitive reaction, the phenyl radicals would abstract

a hydrogen atom from acetonitrile to give cyanomethyl radicals,[45] that would then produce **3**. As far as we are aware, the reactions leading to complexes **2** represent the first instances of intermolecular oxidative additions of a simple iodoarene to Pt(II) that produce stable aryl Pt(IV) complexes.

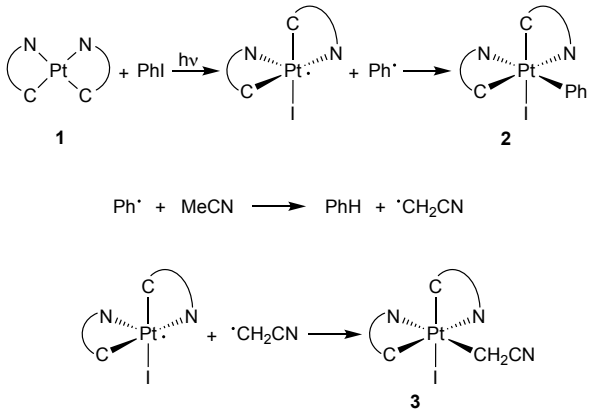

Scheme 2. Proposed radical pathway for the formation of complexes **2** and **3**.

The introduction of aryl ligands was also attempted by reacting precursors **1** with diaryliodonium salts (Scheme 3). These reagents have been previously shown to transfer an aryl cation to M(II) complexes (M = Pd, Pt), with formation of M(IV) species.[46] The reaction of **1b** with $(Ph_2I)PF_6$ in MeCN at room temperature in the dark resulted in a mixture containing a bis-cyclometalated Pt(IV) complex as the major product (*ca.* 83 mol%), as deduced from its ^{1}H NMR data (Fig. S1†). The iodido complexes **2b** and **3b** were also identified as minor products (*ca.* 11 and 6 mol%, respectively). The ESI(+) mass spectrum of the reaction mixture showed the presence of the pentacoordinate cation $[Pt(Ph)(tpy)_2]^+$ at *m/z* 608.1648 as the most abundant ion (calculated *m/z*: 608.1665) and $[Pt(CH_2CN)(tpy)_2]^+$ at *m/z* 571.1449 as a much less abundant species (calculated *m/z*: 571.1461) (Fig. S2†). Therefore, the major species in solution is most probably the solvento complex $[Pt(Ph)(tpy)_2(NCMe)]PF_6$. Since this compound could not be isolated in pure form, it was derivatized by adding γ-picoline (pic), which produced the isolable complex $[PtPh(tpy)_2(pic)]PF_6$ (**4b**; Scheme 3).

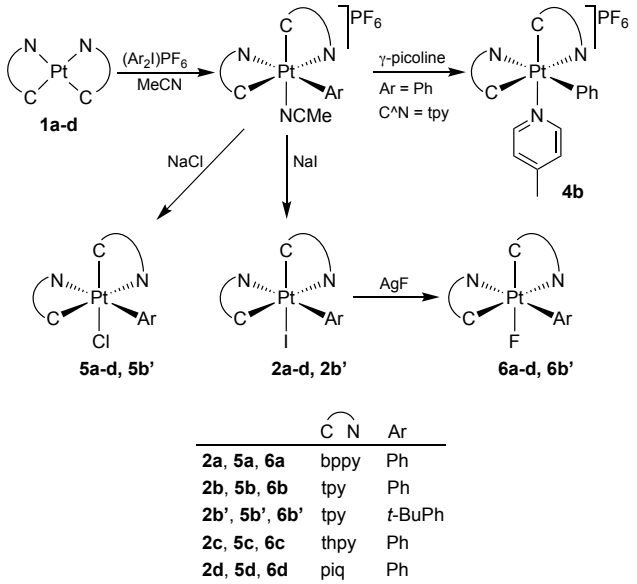

	C N	Ar
2a, **5a**, **6a**	bppy	Ph
2b, **5b**, **6b**	tpy	Ph
2b', **5b'**, **6b'**	tpy	*t*-BuPh
2c, **5c**, **6c**	thpy	Ph
2d, **5d**, **6d**	piq	Ph

Scheme 3. Synthesis of halido(aryl) Pt(IV) complexes.

The formation of complexes **2b** and **3b** along with $[PtPh(tpy)_2(NCMe)]^+$ cations suggests that the reaction between **1b** and Ph_2I^+ involves radicals that can activate iodobenzene and acetonitrile. Possible steps that could explain this result are outlined in Scheme 4. A one-electron reduction of Ph_2I^+ by **1b** would generate a Pt(III) cation complex (**A**), a phenyl radical and iodobenzene. Most of the produced phenyl radicals would couple with species **A** to produce the major cationic product **B**, but some would react with the solvent to give cyanomethyl radicals that, in turn, would couple with **A** to give species **C**. Radical propagation could marginally occur through the reactions of phenyl or cyanomethyl radicals with **1b** to produce the Pt(III) complex **D** and subsequent iodine abstraction from iodobenzene to give **2b** or **3b** and a phenyl radical.

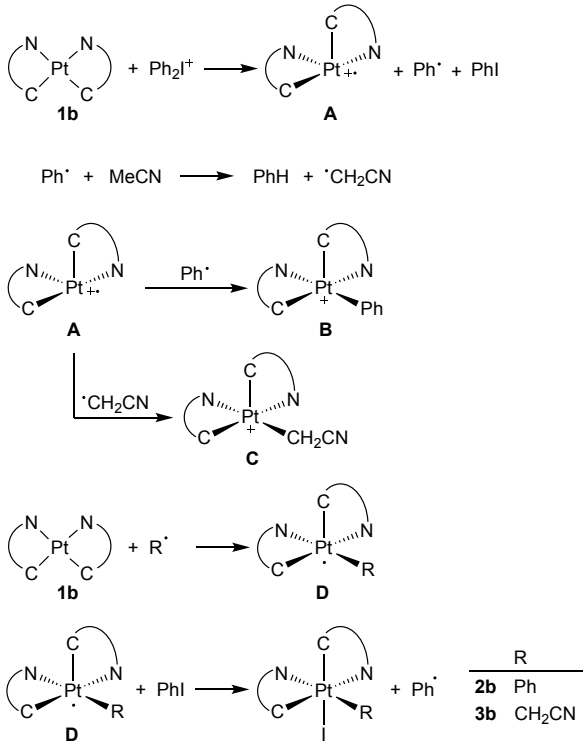

Scheme 4. Proposed steps and intermediates resulting from the reaction of **1b** with Ph_2I^+ in MeCN solution (C^N = tpy).

Since the solvent in $[PtPh(tpy)_2(NCMe)]^+$ can be easily substituted, the addition of a halide salt can lead to bis-cyclometalated halido(aryl) Pt(IV) complexes. Thus, the iodido complexes **2a-d** could be obtained from the reactions the appropriate precursor **1a-d** with $(Ph_2I)PF_6$ in MeCN and subsequent addition of NaI, with similar or somewhat improved yields over the previous method (25–50%). Following the same procedure, the 4-*tert*-butylphenyl derivative $[PtI(t\text{-}BuPh)(tpy)_2]$ (**2b'**) was synthesized by employing $[(t\text{-}BuPh)_2I]PF_6$ and isolated in 65% yield. By using NaCl instead of NaI, the chlorido complexes **5a-d** and **5b'** were obtained as the major products, which needed to be separated from the iodido complexes that form as secondary products by means of column chromatography and were isolated in low yields (19–40%). The fluorido complexes **6a-d** and **6b'** could not be obtained in pure form using this methodology and were synthesized by reacting the corresponding iodido complexes with AgF in CH_2Cl_2 and isolated in good yields (65–78%).

Structural characterization

The unsymmetrical disposition of the C^N ligands in all the new Pt(IV) complexes can be unequivocally determined from the ^{1}H NMR spectra, which show two sets of resonances arising from these ligands. The protons that are closest to the metal are particularly informative because their signals can be flanked by Pt satellites and affected by the diamagnetic ring current of orthogonal aromatic rings (see Fig. 1 for selected spectra). The proton ortho to the metalated carbon of one of the C^N ligands is strongly shielded by the aryl group of the other C^N ligand, appearing in the range 6.70–6.18 ppm. In addition, all the halido(aryl) derivatives give rise to a strongly deshielded aromatic resonance arising from the proton ortho to the N atom of one of the pyridine moieties, which is directed toward the halide. The chemical shift of this resonance was found to depend on the halide, increasing in the sequence F^- (9.13–9.24 ppm) > Cl^- (9.61–9.86 ppm) > I^- (10.08–10.40 ppm) (Fig. 1), and hence it was key for the identification of different halido(aryl) complexes in mixtures. In the case of complex **4b**, this signal appears at a significantly lower chemical shift (8.61 ppm), which can be attributed to the shielding effect of the γ-picoline ring. The aryl protons appear as broad resonances, suggesting restricted rotation, except for the thpy complexes. The cyanomethyl group in complex **3b** gives two characteristic doublets with Pt satellites. The ^{19}F NMR spectra of the fluoride complexes show a resonance in the range from –252.5 to –238.8 ppm with Pt satellites, confirming in all cases the successful substitution of iodide by fluoride.

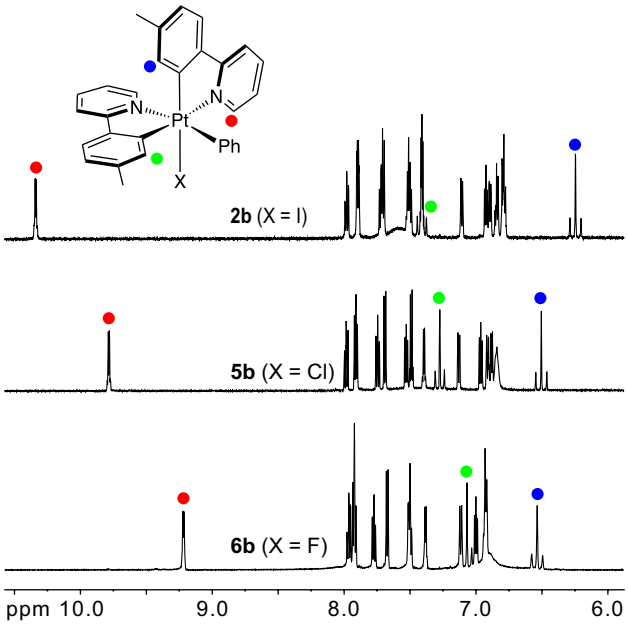

Fig. 1. ^{1}H NMR spectra of complexes **2b**, **5b** and **6b** (CD_2Cl_2, aromatic region). Key resonances are marked with coloured circles.

The structures of **2b**, **4b**·0.5CH_2Cl_2, **5b**, **5b'**·CH_2Cl_2 and **6b**·CH_2Cl_2·H_2O were solved by single-crystal X ray diffraction studies (Fig. 2, Table 1). All of them confirm the unsymmetrical arrangement of the cyclometalated C^N ligands and show that the phenyl group is located trans to the coordinated nitrogen of one of these ligands, whereas the halide or γ-picoline is trans to the metalated carbon of the other one. Complex **6b** presents the shortest Pt–C bond trans to the halido ligand [2.000(4) Å], consistent with the weaker trans influence of fluorido with respect to iodido or chlorido. The Pt–C(Ar) distance is very similar in all the structures (*ca.* 2.04 Å) and slightly longer than Pt–C distances involving the cyclometalated ligands. Complex **6b** crystallized with a water molecule in the asymmetric unit, which is hydrogen-bonded to the fluorido ligand.

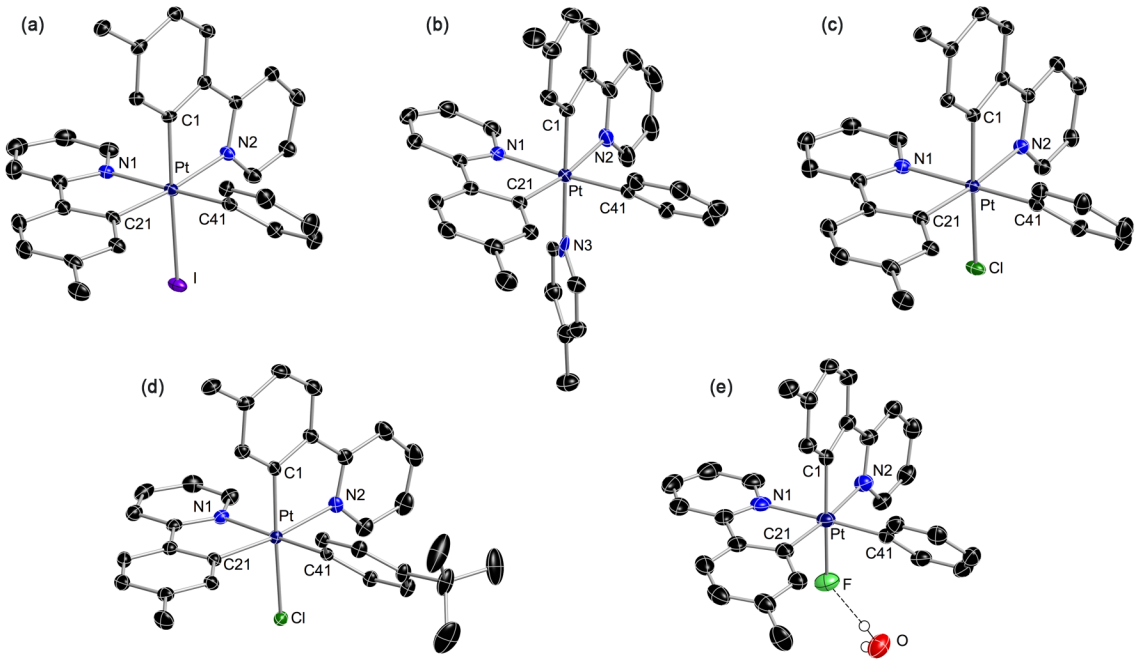

Fig. 2. Structures of **2b** (a), **4b**·0.5CH_2Cl_2 (b), **5b** (c), **5b'**·CH_2Cl_2 (d) and **6b**·CH_2Cl_2·H_2O (e) in the crystal (thermal ellipsoids at 50% probability). Hydrogen atoms, solvent molecules (except for the H_2O molecule of **6b**) and the anion of **4b** are omitted.

Table 1. Selected bond distances (Å) and angles (°) for the crystal structures reported in this work.

	2b	**4b**·0.5CH_2Cl_2	**5b**	**5b'**·CH_2Cl_2	**6b**·CH_2Cl_2·H_2O
Pt–C1	2.029(3)	2.010(3)	2.0133(18)	2.012(3)	2.000(4)
Pt–C21	2.016(3)	2.023(3)	2.0141(18)	2.022(3)	2.007(4)
Pt–C41	2.047(3)	2.044(3)	2.0354(19)	2.042(3)	2.038(4)
Pt–N1	2.137(2)	2.138(2)	2.1386(16)	2.124(2)	2.128(4)
Pt–N2	2.132(2)	2.135(2)	2.1232(15)	2.138(3)	2.116(4)
Pt–X[a]	2.7363(5)	2.231(3)	2.4499(5)	2.4541(7)	2.097(3)
C1–Pt–N2	80.10(10)	80.38(12)	80.31(7)	80.36(11)	80.91(16)
C21–Pt–N1	80.10(10)	80.40(10)	79.98(7)	80.28(11)	80.54(17)

[a] X = I (**2b**), N3 (**4b**), Cl (**5b**, **5b'**) or F (**6b**).

Photophysical Properties

A complete photophysical study has been carried out for the series of complexes **5** and **6** to ascertain the effects of the halide and aryl ligands on their luminescence. Complexes **2** were excluded because they exhibit extremely weak or no emissions due to the detrimental effect of the iodido ligand.[19] The lowest-energy absorption band in CH_2Cl_2 solution shows vibronic structure in all cases (Fig. 3; Table 2) and can be assigned to a singlet excitation primarily localized within the cyclometalated C^N ligand (^{1}LC or $^1\pi$-π^*), as observed for related Pt(IV) complexes.[18] Accordingly, its lowest maximum shifts to longer wavelengths along the series **5a** → **5d** or **6a** → **6d**, as the energies of the lowest π-π* transition of the C^N ligands decrease. The absorption spectra of chlorido and fluorido complexes bearing the same C^N ligand are very similar in shape and energy. However, a close look showed that the lowest-energy slope is slightly red-shifted for the fluorido complexes relative to the chlorido analogues (Fig. S3†). The replacement of the Ph ligand for *t*-BuPh does not produce perceptible changes.

Table 2. Electronic absorption data for the series of complexes **5** and **6** in a CH_2Cl_2 solution (*ca.* 5×10^{-5} M) at 298 K.

Complex	λ_{max} /nm ($\varepsilon \times 10^{-2}$/ M^{-1} cm^{-1})
5a	275 (30.5), 312 (22.8), 329 (20.7)
5b	274 (26.6), 313 (16.8), 325 (16.7), 338 (14.9)
5b'	275 (20.8), 313 (13.5), 326 (13.1), 340 (10.7)
5c	288 (21.2), 346 (15.2)
5d	344 (11.6), 363 (15.2), 378 (13.5)
6a	263 (25.5), 305 (16.0), 319 (13.2), 333 (11.4)
6b	276 (21.7), 312 (13.7), 325 (13.3), 339 (11.9)
6b'	277 (28.2), 313 (18.3), 329 (17.0), 339 (14.9)
6c	291 (20.2), 348 (14.7)
6d	343 (14.7), 365 (17.9), 378 (16.0)

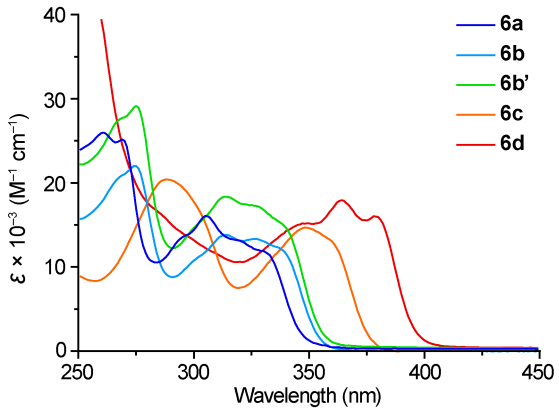

Fig. 3. Electronic absorption spectra of the series of complexes **6** in a CH_2Cl_2 solution at 298 K.

The photoluminescence of the series of complexes **5** and **6** was studied in deaerated CH_2Cl_2 solution and poly(methyl methacrylate) (PMMA) films (2 wt%) at 298 K and in frozen 2-methyltetrahydrofuran glasses at 77 K. The data at 298 K are presented in Table 3 and those at 77 K are given in the ESI.† The emission spectra of the fluorido complexes **6** in fluid CH_2Cl_2 solution are presented in Fig. 4 and a photograph of their luminescence is shown in Fig. 5. The

complete excitation and emission spectra are compiled in the ESI.† All complexes produce a vibronically structured emission band in all media, as typically observed for other cyclometalated Pt(IV) complexes. Excitation spectra faithfully correlate with absorption spectra at 298 K. The chlorido and fluorido derivatives bearing the same C^N ligand exhibit almost identical emission spectra, implying that the halide does not have an appreciable effect on emission energies or spectral shape. Similarly, the replacement of the phenyl ligand in the tpy complexes for *t*-BuPh does not cause any observable variation in the emission spectra. The observed characteristics, together with the long lifetimes in the microsecond range, are evidence of triplet emissive excited states primarily localized on the C^N ligands (^{3}LC).

Table 3. Emission data for the series of complexes **5** and **6** at 298 K.

Complex	Medium	λ_{em}/nm[a]	Φ[b]	τ /μs[c]	$k_r \times 10^{-3}$ /s^{-1} [d]	$k_{nr} \times 10^{-3}$ /s^{-1} [e]
5a	CH_2Cl_2	445, *476*, 505	0.36	124	2.9	5.2
	PMMA	448, *476*, 505	0.79	206	3.8	1.0
5b	CH_2Cl_2	*454*, 484, 514	0.31	130	2.3	5.3
	PMMA	*453*, 485, 513	0.74	273	2.7	1.0
5b'	CH_2Cl_2	*454*, 483, 511	0.42	164	2.6	3.5
	PMMA	*454*, 485, 513	0.88	254	3.5	0.5
5c	CH_2Cl_2	*513*, 529, 551, 599	0.19	146	1.3	5.5
	PMMA	*514*, 531, 553, 600	0.37	233	1.6	2.7
5d	CH_2Cl_2	*564*, 600, 660	0.045	34.6	1.3	27
	PMMA	*561*, 591, 659	0.071	54.5	1.3	17
6a	CH_2Cl_2	448, *478*, 504	0.51	111	4.6	4.4
	PMMA	448, *479*, 504	0.67	149	4.5	2.2
6b	CH_2Cl_2	*455*, 485, 515	0.38	128	2.9	4.8
	PMMA	*454*, 485, 515	0.62	218	2.8	1.7
6b'	CH_2Cl_2	*455*, 486, 515	0.43	125	3.4	4.6
	PMMA	*454*, 485, 515	0.63	199	3.2	1.9
6c	CH_2Cl_2	*516*, 532, 555, 601	0.18	102	1.8	8.0
	PMMA	*516*, 533, 555	0.31	202	1.5	3.4
6d	CH_2Cl_2	*564*, 599	0.044	25.3	1.7	37
	PMMA	*559*, 598, 658	0.071	40.2	1.8	23

[a]Most intense peak in italics. [b]Quantum yield. [c]Emission lifetime. [d]Radiative rate constant, $k_r = \Phi/\tau$. [e]Nonradiative rate constant, $k_{nr} = (1-\Phi)/\tau$.

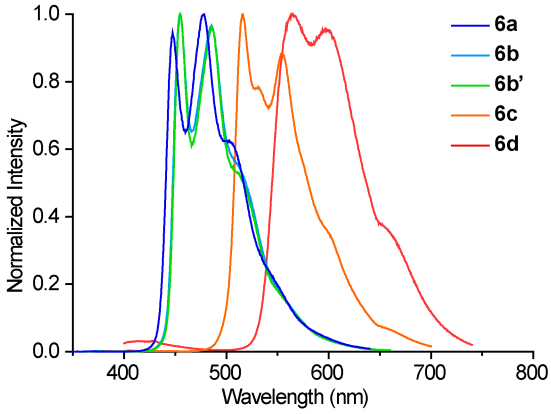

Fig. 4. Emission spectra of the series of complexes **6** in CH_2Cl_2 at 298 K.

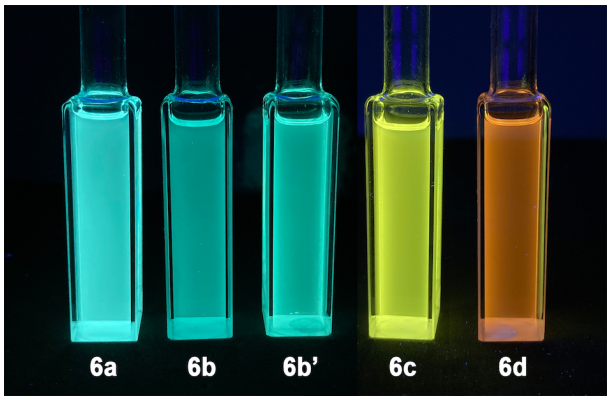

Fig. 5. Luminescence of complexes **6** in CH_2Cl_2 under UV irradiation.

Most of the studied complexes exhibit very bright luminescence, with quantum yields up to 0.51 in CH_2Cl_2 solution (for **6a**) and 0.88 in PMMA (for **5b'**), and thus are amongst the most efficient Pt(IV) emitters. The radiative and nonradiative rate constants (k_r and k_{nr}, respectively) have been calculated assuming that the intersystem crossing to the emissive triplet state has unit efficiency and are given in Table 3. The fluorido derivatives **6** exhibit appreciably shorter emission lifetimes with respect to the chlorido complexes **5**, which are reflected in the higher values found for the $k_r + k_{nr}$ sums. This effect is consistently observed along the whole series, although it does not generally translate into higher quantum yields for the fluorido complexes because the relative increases in k_{nr} can be higher than those in k_r. These larger decay rate constants reveal a more efficient spin-orbit coupling, which is known to increase the transition probabilities of both radiative and nonradiative transitions between states of different spin multiplicities.[47] The effect must be connected to an increased metal orbital involvement in

the excited state for the fluorido derivatives, which is consistent with the computational results (see below).

The piq derivatives **5d** and **6d** are relatively weak emitters, mainly because of their increased k_{nr} values, which are one order of magnitude higher compared with the rest of derivatives. This can be explained on the basis of the lower energy of their emissive excited state, which implies a more effective nonradiative deactivation via vibrational coupling to the ground state, i.e., the Energy-Gap Law.[48] It is also noteworthy that the thpy (**5c**, **6c**) and piq (**5d**, **6d**) derivatives exhibit lower k_r values as compared to the complexes with ppy-based ligands, suggesting a diminished metal orbital contribution to the emissive excited states, probably related to the higher π-orbital energies of the thpy and piq ligands and poorer overlaps with metal dπ orbitals.

The effect of the *t*-BuPh ligand in complexes **5b'** and **6b'** is apparently limited to a decrease in the value of k_{nr} found in CH_2Cl_2 solution, leading to increased quantum yields relative to complexes **5b** and **6b** in this medium. This can be explained by the protective effect of the bulky *t*-Bu group, which may reduce the nonradiative deactivation due to collisions with solvent molecules. In contrast, the variations in k_r are negligible, suggesting that the stronger electron donating capability of the *t*-BuPh ligand is not translated into a perceptible increase in the participation of metal orbitals in the emissive state.

Computational study

DFT and TDDFT calculations have been performed for complexes **5b**, **6b** and **6b'** at the B3LYP/(6-31G**+LANL2DZ) level considering solvent effects (CH_2Cl_2). Full details are given in the ESI.† Frontier molecular orbital energies and selected isosurfaces are represented in Fig. 6. The highest occupied molecular orbital (HOMO) in **5b** is a π(tpy)/dπ(Pt) combination involving the tpy ligand with the N atom trans to the phenyl, with a 6% contribution from metal orbitals, while in **6b** it is a similar combination but with a higher metal orbital involvement (10%) and additional participation of a π orbital from the *p*-tolyl group of the other tpy ligand (Fig. 6). The differences found for the HOMO in **6b** with respect to **5b** correlate with a higher orbital energy in the case of the fluorido complex, indicating a destabilization of dπ orbitals, which is apparently caused by an increased π donation from the *p*-tolyl group trans to the fluorido ligand as a consequence of the shorter Pt–C bond distance. The HOMO in **6b'** is a π(*t*-

BuPh)/dπ(Pt) combination, whereas the HOMO–1 is very similar to the HOMO of **6b**. As expected, the molecular orbitals with a high contribution from the aryl group have lower energies in **5b**/**6b** (HOMO–2) relative to **6b'**. In the three cases, the lowest occupied molecular orbital (LUMO) and the LUMO+1 are π* orbitals of the tpy ligands.

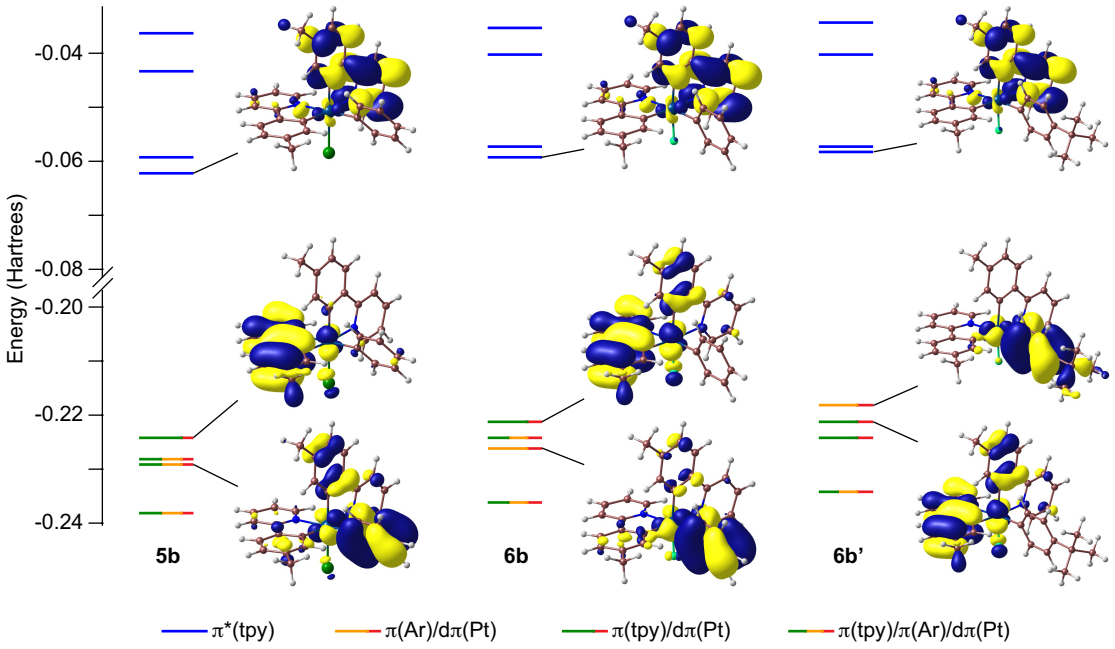

Fig. 6. Molecular orbital energy diagrams and selected isosurfaces (0.03 e bohr^{-3}) from DFT calculations for complexes **5b**, **6b** and **6b'**.

The TDDFT calculations show that the HOMO-LUMO transition is the lowest-energy singlet excitation (S_1) in all cases, corresponding to a predominantly ligand-to-ligand charge-transfer (LLCT) transition between the tpy ligands in **5b** and **6b** or from the *t*-BuPh to one tpy in **6b'**, with very low oscillator strengths. However, the major contribution to the lowest-energy absorption band proceeds from primarily ^{1}LC transitions within the tpy ligands with some MLCT character, which are predicted to be significantly more intense (S_2 and S_3 in **5b**, S_2 in **6b** and S_4 in **6b'**). Their energies are slightly lower for the fluorido complexes **6b** and **6b'** (3.85 eV) relative to the chlorido complex **5b** (3.89 eV), which is consistent with the experimental observations and points to a higher degree of MLCT admixture into the ^{1}LC(tpy) state, as a consequence of the greater metal orbital contribution to the HOMO in the fluorido complexes.

The first two triplet excitations (T_1, T_2) are mainly localized within each of the tpy ligands, the lowest one (T_1) on the ligand with the N atom trans to the aryl group. Hence, the observed luminescence can be attributed to the radiative deexcitation of a ^{3}LC state involving this ligand. The HOMO of **6b'**, comprising π(*t*-BuPh) and dπ(Pt) orbitals, is not involved in the emissive state, which explains why the increased π donation from the *t*-BuPh group does not have an influence on the characteristics of the observed luminescence. The T_1 geometry was optimized for the three studied complexes. The spin density distributions (Fig. 7) correlate with a π-π* transition within the involved tpy ligand, with a non-negligible metal orbital contribution. The natural spin densities on the metal are 0.022 (**5b**) or 0.031 (**6b**, **6b'**), consistent with the higher metal orbital involvement and MLCT admixture into the excited state for the fluorido complexes, which explains their higher decay rate constants.

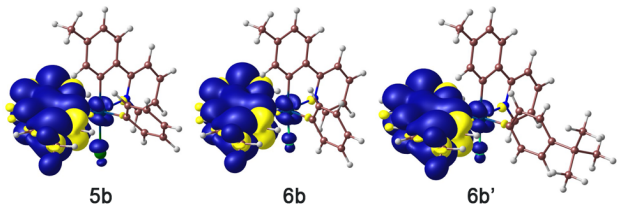

Fig. 7. Spin density distributions (0.001 e bohr^{-3}) of the optimized lowest triplet excited state of **5b**, **6b** and **6b'**.

Conclusions

Two different methodologies have been employed for the synthesis of halido(aryl) Pt(IV) complexes from *cis*-[Pt(C^N)$_2$] precursors. Iodido(phenyl) complexes [PtI(Ph)(C^N)$_2$] were obtained by oxidative addition of iodobenzene in MeCN solution under irradiation with visible light. These reactions constitute the first examples of intermolecular oxidative addition of a simple (non-chelating) aryl halide to Pt(II) that result in stable aryl Pt(IV) complexes. They most probably proceed through radical intermediates, which also engage in a hydrogen abstraction reaction with the solvent to produce variable proportions of cyanomethyl complexes [PtI(CH$_2$CN)(C^N)$_2$]. The introduction of aryl ligands was also achieved by reacting diaryliodonium salts with *cis*-[Pt(C^N)$_2$], which led to cationic intermediates [Pt(Ar)(C^N)$_2$(NCMe)]$^+$ that reacted with iodide or chloride salts to give the corresponding

halido(aryl) complexes. The preparation of the analogous fluorido complexes required a halide exchange reaction from the iodido complexes using AgF.

The effect of the fluorido ligand on the emission properties of this class of compounds has been evaluated by comparing the characteristics of the luminescence of the chlorido and fluorido series. Both series can reach high emission quantum yields at 298 K, but the fluorido complexes consistently showed shorter emission lifetimes and higher decay rates, which indicate a higher MLCT admixture into the primarily ^{3}LC emissive state. The computational results substantiate a higher metal orbital involvement in the excited state for the fluorido complexes, mainly attributable to a stronger π donation from the metalated aryl of the C^N ligand trans to the fluoride. Therefore, the introduction of the fluorido ligand is demonstrated as useful for the modulation of emission lifetimes, which could also be applicable in the design of emissive complexes of other metal ions. In contrast, the increased π donation from the *t*-BuPh ligand relative to the phenyl does not have an influence on the luminescence characteristics of the studied systems.

Experimental section

General considerations, materials, and analytical methods

Unless otherwise noted, all reactions in solution were carried out at room temperature using extra-dry MeCN and flame-dried glassware under an N_2 atmosphere. Synthesis grade Et_2O and CH_2Cl_2 were degassed and dried using a Pure Solv MD-5 solvent purification system from Innovative Technologies, Inc. Other solvents were used as received. Complexes $[Pt_2Me_4(\mu\text{-}SMe_2)_2]$[49] and *cis*-$[Pt(C^N)_2]$[38,39] [C^N = tpy (**1b**), thpy (**1c**) or piq (**1d**)] were prepared following published procedures. Complex *cis*-$[Pt(bppy)_2]$ (**1a**) has not been previously reported and its preparation and characterization are given in the ESI.† All other reagents were obtained from commercial sources. Irradiations were performed using a previously described setup.[38] NMR spectra were registered on Bruker Avance 600, 400 or 300 MHz spectrometers at 298 K. Chemical shifts are referred to residual signals of non-deuterated solvents and are given in ppm downfield from tetramethylsilane. Elemental analyses were carried out with a LECO CHNS-932 microanalyzer. High-resolution electrospray ionization mass spectra (ESI-MS) were recorded on an Agilent 6220 Accurate-Mass time-of-flight (TOF) LC/MS.

General synthesis of [PtI(Ph)(C^N)$_2$] (2). Method A (using PhI): To a solution of the appropriate complex **1** (0.10 mmol) in MeCN (5 mL) was added iodobenzene (0.1 mmol) and the mixture was irradiated with blue light for 4 h. The complexes with C^N = tpy (**2b**) or thpy (**2c**) precipitated from this mixture as white solids, which were collected by filtration, washed with MeCN (3 × 2 mL) and vacuum-dried. The complexes with C^N = bppy (**2a**) or piq (**2d**) did not precipitate and were separated by column chromatography on silica gel, using CH_2Cl_2 as the eluent. In the case of the reaction of **1b** with iodobenzene, the filtrate resulting from the separation of **2b** was chromatographed on silica gel using an AcOEt/hexane (1:1) mixture as the eluent, which allowed the isolation of [PtI(CH_2CN)(tpy)$_2$] (**3b**; yield: 10 mg, 15%).

Method B [using (Ar$_2$I)PF$_6$]: To a suspension of the appropriate complex **1** (0.18 mmol) in MeCN (5 mL) was added (Ar$_2$I)PF$_6$ (0.18 mmol) and the mixture was stirred for 4 h, whereupon a colourless solution was obtained. The solvent was removed under reduced pressure and a solution of NaI (1 mmol) in acetone (20 mL) was added. The resultant suspension was stirred for 6 h and evaporated to dryness. The residue was treated with CH_2Cl_2 (20 mL) and the suspension was filtered through Celite. The filtrate was concentrated to *ca.* 1 mL and passed through silica gel in a chromatography column using CH_2Cl_2. Partial evaporation of the resulting solution (1 mL) and addition of Et_2O (15 mL) led to the precipitation of a white or pale yellow solid, which was collected by filtration, washed with Et_2O (3 × 2 mL) and vacuum-dried to give the corresponding complex **2**.

Table 4. Isolated yields (%) of complexes **2**.

Complex	Method A	Method B
2a	47	50
2b	38	45
2b'	–	65
2c	40	46
2d	30	25

[PtI(Ph)(bppy)$_2$] (2a). White solid. ^{1}H NMR (400 MHz, CD_2Cl_2): δ 10.23 (d with satellites, J_{HH} = 6.1 Hz, J_{PtH} = 15.0 Hz, 1H), 7.92 (s, 2H), 7.89-7.80 (m, 1H), 7.66-7.49 (m, 5H), 7.48-7.38 (d with satellites, J_{HH} = 7.4 Hz, J_{PtH} = 15 Hz, 1H), 7.35-7.23 (m, 2H), 7.08 (ddd, J_{HH} = 8.7, 7.5, 1.3 Hz, 1H), 7.03-6.92 (m, 2H), 6.89-6.73 (m, 3H), 6.45 (dd with satellites, J_{HH} = 8.05, 1.2 Hz, J_{PtH} = 50.0 Hz, 1H), 1.44 (s, 9H), 1.31 (s, 9H). ^{13}C{^{1}H} NMR (150.8 MHz, CD_2Cl_2): δ 164.7 (C), 163.8 (C), 162.4 (J_{PtC} = 50.4 Hz, C), 161.4 (J_{PtC} = 54.3 Hz, C), 151.6 (CH), 148.2 (J_{PtC} = 877.3 Hz, C), 146.4 (CH), 143.2 (J_{PtC} = 888.0 Hz, C), 142.3 (C), 141.2 (C), 134.3 (J_{PtC}

= 59.3 Hz, CH), 131.7 (J_{PtC} = 59.3 Hz, CH), 130.2 (J_{PtC} = 47.3 Hz, CH), 129.3 (J_{PtC} = 852.3 Hz, C), 127.1 (J_{PtC} = 51.0 Hz, CH), 125.4 (CH), 125.2 (CH), 125.0 (CH), 124.9 (CH), 124.1 (CH), 123.4 (CH), 121.3 (CH), 117.6 (CH), 36.0 (C), 35.8 (C), 30.73 ($3CH_3$), 30.65 ($3CH_3$). Elemental analysis calcd (%) for $C_{36}H_{37}N_2IPt$: C 52.75, H 4.55, N 3.42; found: C 52.79, H 4.33, N 3.46.

[PtI(Ph)(tpy)$_2$] (2b). White solid. ^{1}H NMR (600 MHz, CD_2Cl_2): δ 10.34 (ddd with satellites, J_{HH} = 5.6, 1.7, 0.8 Hz, J_{PtH} = 15.0 Hz, 1H), 7.98 (ddd, J = 8.2, 7.4, 1.6 Hz, 1H), 7.92-7.87 (m, 2H), 7.75-7.68 (m, 2H), 7.67-7.48 (m, 5H), 7.46-7.36 (m, 2H), 7.11 (d, J = 8.2 Hz, 1H), 6.95-6.76 (m, 4H), 6.24 (s with satellites, J_{PtH} = 50.2 Hz, 1H), 2.38 (s, 3H), 2.11 (s, 3H). The ^{13}C NMR spectrum of this compound could not be registered because of its very low solubility. Elemental analysis calcd (%) for $C_{30}H_{25}N_2IPt \cdot 0.25H_2O$: C 48.99, H 3.43, N 3.81; found: C 48.69, H 3.47, N 3.79.

[PtI(*t*-BuPh)(tpy)$_2$] (2b'). White solid. ^{1}H NMR (400 MHz, CD_2Cl_2): δ 10.34 (d, J = 5.5 Hz, 1H), 7.98 (ddd, J = 8.3, 7.5, 1.7 Hz, 1H), 7.93-7.82 (m, 2H), 7.75-7.64 (m, 2H), 7.58-7.34 (m, 6H), 7.10 (dd, J = 8.3, 1.8 Hz, 1H), 6.98-6.77 (m, 4H), 6.25 (s with satellites, J_{PtH} = 50.4 Hz, 1H), 2.40 (s, 3H), 2.11 (s, 3H), 1.22 (s, 9H). ^{13}C{^{1}H} NMR (150.8 MHz, CD_2Cl_2): δ 163.1 (J_{PtC} = 52.0 Hz, C), 162.1 (J_{PtC} = 51.7 Hz, C), 152.2 (CH), 148.1 (J_{PtC} = 886.0 Hz, C), 146.6 (CH), 142.8 (J_{PtC} = 890.8 Hz, C), 142.6 (J_{PtC} = 55.1 Hz, C), 142.5 (J_{PtC} = 62.9 Hz, C), 139.8 (CH), 139.4 (C), 139.1 (CH), 138.2 (C), 134.7 (J_{PtC} = 43.4 Hz, CH), 130.8 (J_{PtC} = 51.0 Hz, CH), 126.5 (CH), 126.0 (CH), 125.2 (CH), 125.1 (CH), 125.06 (J_{PtC} = 856.0 Hz, C), 124.3 (J_{PtC} = 52.0 Hz, CH), 123.0 (CH), 120.5 (CH), 120.4 (CH), 34.3 (C), 31.7 ($3CH_3$), 22.3 (CH_3), 22.1 (CH_3). Elemental analysis calcd (%) for $C_{34}H_{33}IN_2Pt$: C 51.59, H 4.20, N 3.54; found: C 51.66, H 4.35, N 3.48.

[Pt(thpy)$_2$I(Ph)] (2c). Pale yellow solid. ^{1}H NMR (600 MHz, CD_2Cl_2): δ 10.08 (ddd with satellites, J_{HH} = 5.6, 1.7, 0.8 Hz, J_{PtH} = 15 Hz, 1H), 7.94 (ddd, J = 8.0, 7.5, 1.6 Hz, 1H), 7.68 (td, J = 8.1, 1.6 Hz, 1H), 7.61 (d with satellites, J_{HH} = 5.1 Hz, J_{PtH} = 15.1 Hz, 1H), 7.60-7.56 (m, 2H), 7.54 (d with satellites, J_{HH} = 5.2 Hz, J_{PtH} = 15.6 Hz, 1H), 7.47 (d with satellites, J_{HH} = 5.2 Hz, J_{PtH} = 48.0 Hz, 2H), 7.39 (td, J = 8.1, 1.6 Hz, 1H), 7.25 (d with satellites, J_{HH} = 5.2 Hz, J_{PtH} = 15.6 Hz, 2H), 7.20 (d with satellites, J_{HH} = 5.2 Hz, J_{PtH} = 15.6 Hz, 1H), 6.90-6.79 (m, 3H), 6.18 (d with satellites, J_{HH} = 5.4 Hz, J_{PtH} = 17.6 Hz, 1H). The ^{13}C NMR spectrum of this compound could not be measured because of its very low solubility. Elemental analysis calcd (%) for $C_{24}H_{17}N_2IPt$: C 40.06, H 2.38, N 3.89, S 8.91; found: C 40.05, H 2.37, N 3.54, S 8.44.

[PtI(piq)$_2$(Ph)] (2d). Pale yellow solid. ^{1}H NMR (400 MHz, CD_2Cl_2): δ 10.40 (d with satellites, J_{HH} = 6.2 Hz, J_{PtH} = 14.0 Hz, 1H), 8.96 (m, 1H), 8.72 (d, J = 8.7, 1H), 8.35 (dd with satellites, J_{HH} = 7.7, 2.0 Hz, J_{PtH} = 7.3 Hz, 1H), 8.07 (d, J_{HH} = 8.3 Hz, 1H), 7.97 (d with satellites, J_{HH} = 8.1 Hz, J_{PtH} = 9.0 Hz, 1H), 7.92 (d, J = 6.4 Hz, 1H), 7.87 (ddd, J = 8.1, 6.9, 1.1 Hz, 1H), 7.83-7.65 (m, 7H), 7.58 (d with satellites, J_{PtH} = 8.4 Hz, 1H), 7.43-7.30 (m, 2H), 7.24 (dd, J = 6.3, 0.9 Hz, 1H), 7.09 (ddd, J = 8.0, 7.3, 1.3 Hz, 1H), 6.96 (ddd, J = 8.0, 7.3, 1.3 Hz, 1H), 6.84-6.70 (m, 4H). The ^{13}C NMR spectrum of this compound could not be measured because of its very low solubility. Elemental analysis calcd (%) for $C_{36}H_{25}N_2IPt\cdot0.5CH_2Cl_2$: C 51.57, H 3.08, N 3.30; found: C 51.04, H 2.79, N 3.41.

[PtI(CH$_2$CN)(tpy)$_2$] (3b). White solid. ^{1}H NMR (600 MHz, CD_2Cl_2): δ 10.21 (d with satellites, J_{HH} = 5.4 Hz, J_{PtH} = 14.9 Hz, 1H), 8.10-8.04 (m, 2H), 7.90 (d, J = 8.2 Hz, 1H), 7.74 (ddd, J = 8.3, 7.3, 1.6 Hz, 1H), 7.69 (d, J = 7.9 Hz, 1H), 7.59-7.55 (m, 1H), 7.54 (ddd, J = 7.2, 5.6, 1.8 Hz, 1H), 7.49 (d with satellites, J_{HH} = 6.0 Hz, J_{PtH} = 19.1 Hz, 1H), 7.24 (s with satellites, J_{PtH} = 37.2 Hz, 1H), 7.16 (d, J = 7.7 Hz, 1H), 6.96-6.91 (m, 2H), 6.04 (s with satellites, J = 50.6 Hz, 1H), 3.07 (d with satellites, J_{HH} = 14.1 Hz, J_{PtH} = 106.4 Hz, 1H), 2.54 (d with satellites, J_{HH} = 14.1 Hz, J_{PtH} = 78.9 Hz, 1H), 2.52 (s, 3H), 2.07 (s, 3H). ^{13}C{^{1}H} NMR (150.8 MHz, CD_2Cl_2): δ 163.2 (J_{PtC} = 56.4 Hz, C), 162.3 (J_{PtC} = 59.9 Hz, C), 152.5 (CH), 147.1 (CH), 145.5 (C), 143.4 (J_{PtC} = 49.6 Hz, C), 142.7 (J_{PtC} = 60.3 Hz, C), 140.6 (C), 140.3 (CH), 139.5 (CH), 138.6 (C), 131.2 (J_{PtC} = 48.8 Hz, CH), 130.4 (J_{PtC} = 34.7 Hz, CH), 127.1 (CH), 126.5 (CH), 125.6 (CH), 123.3 (CH), 123.1 (C), 120.9 (J_{PtC} = 15.1 Hz, CH), 120.7 (J_{PtC} = 19.6 Hz, CH), 22.4 (CH_3), 22.0 (CH_3); (*C*H$_2$ and *C*N not observed). Elemental analysis calcd (%) for $C_{26}H_{22}N_3IPt$: C 44.71, H 3.17, N 6.02; found: C 44.59, H 3.11, N 6.01.

Synthesis of [Pt(Ph)(tpy)$_2$(pic)]PF$_6$ (4b). To a suspension of **1b** (45 mg, 0.09 mmol) in MeCN (5 mL) was added $(Ph_2I)PF_6$ and mixture was stirred for 4 h, whereupon a colourless solution was obtained. γ-Picoline (100 μL, 1 mmol) was then added and the solution was stirred for 5 min. The solvent was removed under reduced pressure and the residue was chromatographed on silica gel using a $CHCl_3$/MeOH mixture (15:1) as the eluent. Partial evaporation of the solvent (1 mL) and addition of Et_2O (20 mL) led to the precipitation of a white solid, which was collected by filtration, washed with Et_2O (3 × 2 mL) and vacuum-dried to give **4b**. Yield: 30 mg, 42%. ^{1}H NMR (401 MHz, CD_2Cl_2): δ 8.61 (d, J = 5.3 Hz, 1H), 8.23 (d with satellites, J_{HH} = 6.2 Hz, J_{PtH} = 10.5 Hz, 2H), 8.10 (dt, J = 8.0, 1.6 Hz, 1H), 7.97 (d, J = 8.4 Hz, 1H), 7.92-7.85 (m, 2H), 7.69 (dt, J_{HH} = 5.5, 1.3 Hz, 1H), 7.62 (td, J_{HH} = 5.8, 1.42 Hz, 1H), 7.59 (d, J_{HH} =

7.9 Hz, J_{PtH} = 8.1 Hz, 1H), 7.1 (s with satellites, 39.6 Hz, J_{PtH} = 13.9 Hz, 1H), 7.47 (d, J_{HH} = 8.0 Hz, J_{PtH} = 8.4 Hz, 1H), 7.31-7.20 (m, 3H), 7.20-7.06 (m, 3H), 7.06-6.97 (m, 1H), 6.97-6.87 (m, 3H), 6.51 (s with satellites J_{PtH} = 45.2 Hz, 1H), 2.41 (s, 3H), 2.37 (s, 3H), 2.15 (s, 3H). $^{13}C\{^1H\}$ NMR (150.8 MHz, CD_2Cl_2): δ 162.6 (J_{PtC} = 48.2 Hz, C), 162.4 (J_{PtC} = 51.7 Hz, C), 153.4 (C), 150.6 (CH), 146.9 (CH), 146.7 (CH), 143.9 (C), 143.7 (C), 143.6 (C), 141.3 (CH), 141.0 (CH), 139.5 (C), 138.4 (C), 138.2 (C), 136.0 (CH), 133.1 (J_{PtC} = 50.1 Hz, CH), 132.9 (J_{PtC} = 44.1 Hz, CH), 131.4 (C), 128.3 (J_{PtC} = 50.0 Hz, CH), 127.5 (CH), 127.3 (CH), 126.0 (J_{PtC} = 34.5 Hz, CH), 125.6 (CH), 125.3 (J_{PtC} = 35.2 Hz, CH), 121.3 (CH), 121.1 (CH), 22.4 (CH_3), 22.1 (CH_3), 21.6 (CH_3). ^{19}F NMR (282 MHz, CD_2Cl_2): δ –73.1 (d, J_{PF} = 705.4 Hz). Elemental analysis calcd (%) for $C_{37}H_{32}N_3PF_6Pt$: C 51.07, H 3.81, N 4.96; found: C 50.65, H 3.72, N 4.78.

General procedure for the synthesis of [PtCl(Ar)(C^N)$_2$] (5). To a suspension of the appropriate complex **1** (0.19 mmol) in MeCN (5 mL) was added the $(Ar_2I)PF_6$ salt and the mixture was stirred for 4 h, whereupon a colourless solution was obtained. The solvent was removed under reduced pressure and a suspension of NaCl (1 mmol) in acetone (20 mL) was added. The resultant suspension was stirred for 6 h, the solvent was evaporated under reduced pressure and the residue was chromatographed on silica gel using CH_2Cl_2 as the eluent. Partial evaporation of the solvent (1 mL) and addition of Et_2O (10 mL) led to the precipitation of a white solid, which was collected by filtration, washed with Et_2O (3 × 2 mL) and vacuum-dried to give the corresponding complex **5**.

[PtCl(Ph)(bppy)$_2$] (5a). White solid, obtained from **1a** (50 mg. 0.08 mmol) and $(Ph_2I)PF_6$ (35 mg, 0.08 mmol). Yield: 17 mg, 30%. ^1H NMR (401 MHz, CD_2Cl_2): δ 9.67 (dd with satellites, J_{HH} = 6.1, 0.7 Hz, J_{PtH} = 14.9 Hz, 1H), 7.95 (d, J = 2.1 Hz, 2H), 7.84 (dd, J = 7.7 Hz, 1H), 7.69-7.62 (m, 1H), 7.59 (dd, J = 6.1, 2.0 Hz, 1H), 7.43 (dd with satellites, J_{HH} = 7.80, 2.15 Hz, J_{PtH} = 41.16 Hz, 2H), 7.36-7.21 (m, 3H), 7.14-7.06 (m, 1H), 7.04 (dd, J = 6.0, 2.0 Hz, 1H), 6.98-6.91 (m, 1H), 6.91-6.79 (m, 4H), 6.69 (d with satellites, J_{HH} = 7.9 Hz, J_{PtH} = 49.6 Hz, 1H), 1.45 (s, 9H), 1.31 (s, 9H). $^{13}C\{^1H\}$ NMR (150.8 MHz, CD_2Cl_2): δ 165.0 (C), 164.0 (C), 162.3 (C), 161.8 (J_{PtC} = 53.0 Hz, C), 147.5 (CH), 145.9 (CH), 144.7 (C), 144.6 (C), 142.7 (C), 141.2 (C), 133.8 (J_{PtC} = 41.6 Hz, CH), 132.1 (CH), 132.0 (CH), 131.8 (CH), 131.0 (C), 127.3 (J_{PtC} = 50.3 Hz, CH), 125.22 (CH), 125.20 (CH), 125.1 (CH), 125.0 (CH), 124.3 (CH), 123.3 (CH), 122.4 (CH), 121.4 (CH), 119.6 (CH), 117.6 (J_{PtC} = 14.2 Hz, CH), 117.4 (J_{PtC} = 14.2 Hz, CH), 36.0

(C), 35.8 (C), 30.7 ($3CH_3$), 30.6 ($3CH_3$). Elemental analysis calcd (%) for $C_{35}H_{37}N_2ClPt$: C 59.38, H 5.12, N 3.85; found: C 58.86, H 4.99, N 3.71.

[PtCl(Ph)(tpy)$_2$] (5b). White solid, obtained from **1b** (100 mg. 0.18 mmol) and $(Ph_2I)PF_6$ (80 mg, 0.18 mmol). Yield: 45 mg, 40%. ^{1}H NMR (600 MHz, CD_2Cl_2): δ 9.78 (ddd with satellites, J_{HH} = 5.6, 1.7, 0.9 Hz, J_{PtH} = 15.0 Hz, 1H), 8.02-7.95 (m, 1H), 7.94-7.86 (m, 2H), 7.78-7.71 (m, 1H), 7.69 (d, J = 7.9, Hz, 1H), 7.54 (td, J = 5.8, 1.2 Hz, 1H), 7.51-7.47 (m, 1H), 7.39 (ddd, J_{HH} = 5.6, 1.7, 0.9 Hz 1H), 7.27 (s with satellites, J_{PtH} = 41.2 Hz, 1H), 7.13 (ddd, J = 7.9, 1.4, 0.7 Hz, 1H), 6.96 (td, J = 5.8, 1.2 Hz, 1H), 6.94-6.79 (m, 6H), 6.50 (s with satellites, J_{PtH} = 50.5 Hz, 1H), 2.35 (s, 3H), 2.12 (s, 3H). The ^{13}C NMR spectrum of this compound could not be registered because of its very low solubility. Elemental analysis calcd (%) for $C_{30}H_{25}N_2ClPt\cdot 0.3CH_2Cl_2$: C 54.19, H 3.85, N 4.17; found: C 54.07, H 3.82, N 4.10.

[PtCl(*t*-BuPh)(tpy)$_2$] (5b'). White solid, obtained from **1b** (65 mg. 0.12 mmol) and [(*t*-BuPh)$_2$I]PF_6 (66 mg, 0.12 mmol). Yield: 23 mg, 28%. ^{1}H NMR (600 MHz, CD_2Cl_2): δ 9.80 (d with satellites, J_{HH} = 5.37 Hz, J_{PtH} = 15.0 Hz, 1H), 7.99 (ddd, J = 8.2, 7.4, 1.6 Hz, 1H), 7.90 (td, J = 6.8, 1.1 Hz, 2H), 7.73 (ddd, J = 8.2, 7.4, 1.6 Hz, 1H), 7.68 (d, J = 8.27 Hz, 1H), 7.53 (ddd, J = 7.5, 5.6, 1.3 Hz, 1H), 7.51-7.47 (m, 1H), 7.40-7.32 (m, 4H), 7.13 (d, J = 7.98 Hz, 1H), 6.98-6.92 (m, 1H), 6.92-6.88 (m, 3H), 6.51 (s with satellites, J_{PtH} = 50 Hz, 1H), 2.37 (s, 3H), 2.12 (s, 3H), 1.22 (s, 9H). ^{13}C{^{1}H} NMR (150.8 MHz, CD_2Cl_2): δ 163.0 (C), 162.5 (C), 148.1 (CH), 146.8 (C), 146.1 (CH), 144.5 (J_{PtC} = 914.3 Hz, C), 144.4 (J_{PtC} = 899.5 Hz, C), 142.7 (C), 142.6 (C), 140.2 (CH), 139.7 (C), 139.2 (CH), 138.1 (C), 135.6 (CH), 134.4 (J_{PtC} = 42.2 Hz, CH), 132.7 (CH), 126.7 (J_{PtC} = 863.7 Hz, C), 126.2(CH), 126.1(CH), 125.3 (J_{PtC} = 34.8 Hz, CH), 125.1 (J_{PtC} = 37.8 Hz, CH), 124.32 (J_{PtC} = 49.6 Hz, CH), 123.1 (CH), 120.3 (CH), 120.2 (CH), 34.4 (C), 31.7 ($3CH_3$), 22.28 (CH_3), 22.03 (CH_3). Elemental analysis calcd (%) for $C_{34}H_{33}N_2ClPt\cdot 0.5CH_2Cl_2$: C 55.80, H 4.61, N 3.77; found: C 54.80, H 4.66, N 4.04.

[PtCl(Ph)(thpy)$_2$] (5c). White solid, obtained from **1c** (103 mg. 0.20 mmol) and $(Ph_2I)PF_6$ (85 mg, 0.20 mmol). Yield: 23 mg, 19%. ^{1}H NMR (400 MHz, CD_2Cl_2): δ 9.61 (d with satellites, J_{HH} = 5.5 Hz, J_{PtH} = 16.7 Hz, 1H), 7.95 (td, J = 7.8, 1.6 Hz, 1H), 7.71 (td, J = 8.1, 1.5 Hz, 1H), 7.63-7.53 (m, 3H), 7.47-7.40 (m, 2H), 7.32 (d with satellites, J_{HH} = 7.3 Hz, J_{PtH} = 47.0 Hz, 1H), 7.26 (d with satellites, J_{HH} = 4.9 Hz, J_{PtH} = 10.6 Hz, 2H), 7.14 (d with satellites, J_{HH} = 5.2 Hz, J_{PtH} = 15.5 Hz, 1H), 6.97-6.81 (m, 4H), 6.29 (d with satellites, J_{HH} = 5.2 Hz, J_{PtH} = 18.6 Hz, 1H). The ^{13}C NMR spectrum of this compound could not be registered because of its very low

solubility. Elemental analysis calcd (%) for $C_{24}H_{17}N_2ClS_2Pt$: C 45.90, H 2.73, N 4.46, S 10.21; found: C 46.08, H 2.54, N 4.58, S 10.10.

[PtCl(Ph)(piq)$_2$] (5d). White solid, obtained from **1d** (104 mg. 0.17 mmol) and $(Ph_2I)PF_6$ (74 mg, 0.17 mmol). Yield: 25 mg, 21%. ^{1}H NMR (400 MHz, CD_2Cl_2): δ 9.86 (d with satellites, J_{HH} = 6.35, J_{PtH} = 8.2 Hz, 1H), 9.02-8.95 (m, 1H), 8.82 (d, J = 8.7 Hz, 1H), 8.33 (d, J = 8.9 Hz, 1H), 8.13 (m, 1H), 8.06 (d, J = 8.2 Hz, 1H), 7.95 (d, J = 6.3 Hz, 1H), 7.87 (t, J = 7.5 Hz, 1H), 7.83-7.71 (m, 4H), 7.57 (d with satellites, J_{HH} = 8.0 Hz, J_{PtH} = 43.0 Hz, 1 H), 7.53-7.37 (m, 4H), 7.37-7.25 (m, 2H), 7.18-7.08 (m, 1H), 7.01-6.87 (m, 2H), 6.87-6.76 (m, 3H). The ^{13}C NMR spectrum of this compound could not be registered because of its very low solubility. Elemental analysis calcd (%) for $C_{36}H_{25}N_2ClPt{\cdot}H_2O{\cdot}CH_2Cl_2$: C 54.19, H 3.19, N 3.68; found: C 54.26, H 3.57, N 3.42.

General procedure for the synthesis of [PtF(Ph)(C^N)$_2$] (6). To a solution of corresponding iodide complex **2** in CH_2Cl_2 (40 mL) was added AgF (5 eq) and the resulting suspension was stirred for 24 h and then filtered through Celite. The filtrate was concentrated under reduced pressure (1 mL) and pentane (15 mL) was added, whereupon a white or pale yellow solid precipitated, which was collected by filtration, washed with Et_2O (3 × 2 mL) and vacuum-dried to give the corresponding complex **6**.

[PtF(Ph)(bppy)$_2$] (6a). White solid, obtained from **2a** (76 mg. 0.09 mmol) and AgF (23 mg, 0.18 mmol). Yield: 43 mg, 65%. ^{1}H NMR (400 MHz, CD_2Cl_2): δ 9.13 (d with satellites, J_{HH} = 6.3 Hz, J_{PtH} = 13.5 Hz, 1H), 7.96 (dd, J = 4.8, 2.0 Hz, 2H), 7.82 (dd, J = 7.8, 1.5 Hz, 1H), 7.67 (d, J = 7.9 Hz, 1H), 7.56 (dd, J = 5.9, 1.9 Hz, 1H), 7.34-7.24 (m, 3H), 7.24-7.14 (m, 2H), 7.14-7.04 (m, 2H), 6.98-6.81 (m, 5H), 6.70 (dd with satellites, J_{HH} = 8.3, 2.6 Hz, J_{PtH} = 48.5 Hz, 1H), 1.44 (s, 9H), 1.31 (s, 9H). ^{13}C{^{1}H} NMR (150.8 MHz, CD_2Cl_2): δ 165.1 (C), 164.4 (C), 162.7, (J_{PtC} = 50.3 Hz, C), 161.3 (J_{PtC} = 54.0 Hz, C), 146.22 (CH), 146.18 (CH), 145.8 (CH), 145.6 (C), 143.4 (C), 141.6 (C), 136.4 (d, J_{CF} = 50.5 Hz, C), 134.1 (J_{PtC} = 45.3 Hz, CH), 133.6 (J_{PtC} = 45.3 Hz, CH), 133.0 (J_{PtC} = 870.1 Hz, C), 131.6 (J_{PtC} = 57.9 Hz, CH), 131.5 (CH), 127.5 (CH), 127.3 (CH), 125.2 (CH), 125.1 (CH), 124.9 (CH), 124.74 (CH), 124.55 (CH), 121.8 (CH), 121.5 (CH), 117.4 (J_{PtC} = 14.2 Hz, CH), 117.3 (J_{PtC} = 15.5 Hz, CH), 36.0 (C), 35.8 (C), 30.81 ($3CH_3$), 30.61 ($3CH_3$). ^{19}F NMR (282 MHz, CD_2Cl_2): δ –245.0 (s with satellites, J_{PtF} = 50.2 Hz). Elemental analysis calcd (%) for $C_{36}H_{37}N_2FPt$: C 60.75, H 5.24, N 3.94; found: C 60.62, H 5.31, N 3.60.

[PtF(Ph)(tpy)$_2$] (6b). White solid, obtained from **2b** (50 mg. 0.07 mmol) and AgF (18 mg, 0.14 mmol). Yield: 25mg, 59%. ^{1}H NMR (600 MHz, CD_2Cl_2): δ 9.22 (d with satellites, J_{HH} = 5.0 Hz, J_{PtH} = 13.4 Hz, 1H), 8.00-7.90 (m, 4H), 7.77 (ddd, J = 8.2, 7.4, 1.6 Hz, 1H), 7.67 (d, J = 7.9 Hz, 1H), 7.53-7.48 (m, 2H), 7.38 (d with satellites, J_{HH} = 5.0 Hz, J_{PtH} = 13.4 Hz, 1H), 7.11 (d, J_{HH} = 7.2 Hz, 1H), 7.07 (s with satellites, J_{PtH} = 40.7 Hz, 1H), 7.00 (ddd, J = 8.5, 5.6, 1.2 Hz, 1H), 6.98-6.75 (m, 5H), 6.54 (s with satellites, J_{PtH} = 49.6 Hz, 1H), 2.30 (s, 3H), 2.12 (s, 3H). ^{13}C{^{1}H} NMR (150.8 MHz, CD_2Cl_2): δ 163.5 (C), 162.0 (C), 146.79 (CH), 146.75 (CH), 146.3 (CH), 145.3 (C), 142.3 (C), 140.3 (CH), 139.7 (CH), 138.4 (C), 136.3 (d, J_{CF} = 48.2 Hz, C), 134.9 (J_{PtC} = 45.4 Hz, CH), 134.1 (J_{PtC} = 45.4 Hz, CH), 132.6 (C), 127.4 (CH), 126.3 (CH), 126.0 (CH), 125.9 (CH), 125.3 (CH), 125.1 (CH), 124.6 (CH), 123.7 (CH), 123.2 (CH), 120.2 (J_{PtC} = 14.1 Hz, CH), 120.0 (J_{PtC} = 15.5 Hz, CH), 22.2 (CH_3), 21.0 (CH_3). ^{19}F NMR (282 MHz, CD_2Cl_2): δ –243.3 (s with satellites, J_{PtF} = 71.6 Hz). Elemental analysis calcd (%) for $C_{30}H_{25}FN_2Pt{\cdot}0.5CH_2Cl_2$: C 54.67, H 3.91, N 4.18; found: C 54.60, H 4.12, N 4.55.

[PtF(*t*-BuPh)(tpy)$_2$] (6b'). White solid, obtained from **2b'** (56 mg. 0.07 mmol) and AgF (18 mg, 0.14 mmol). Yield: 37 mg, 74%. ^{1}H NMR (400 MHz, CD_2Cl_2): δ 9.23 (d, J_{HH} = 5.6 Hz, 1H), 8.02-7.87 (m, 3H), 7.76 (td, J = 7.8, 1.6 Hz, 1H), 7.66 (d, J_{HH} = 7.9 Hz, 1H), 7.55-7.46 (m, 2H), 7.35 (d, J_{HH} = 5.6 Hz, 1H), 7.18-7.02 (m, 2H), 7.02-6.87 (m, 6H), 6.54 (s with satellites, J_{PtH} = 49.8 Hz, 1H), 2.31 (s, 3H), 2.12 (s, 3H), 1.23 (s, 9H). ^{13}C{^{1}H} NMR (150.8 MHz, CD_2Cl_2): δ 163.5 (C), 162.1 (C), 147.1 (C), 146.9 (CH), 146.2 (CH), 145.5 (C), 142.3 (C), 140.4 (C), 140.3 (CH), 139.7 (CH), 138.5 (C), 136.3 (d, J_{CF} = 50.5 Hz, C), 134.9 (J_{PtC} = 47.7 Hz, CH), 134.3 (J_{PtC} = 46.9 Hz, CH), 133.7 (CH), 132.6 (CH), 128.7 (C), 126.2 (CH), 125.8 (CH), 125.2 (J_{PtC} = 31.5 Hz, CH), 125.0 (J_{PtC} = 34.9 Hz, CH), 124.5 (J_{PtC} = 49.6 Hz, CH), 123.7 (CH), 123.2 (CH), 120.2 (CH), 120.0 (J_{PtC} = 15.1 Hz, CH), 34.3 (C), 31.73 (3CH_3), 22.19 (CH_3), 21.95 (CH_3). ^{19}F NMR (282 MHz, CD_2Cl_2): δ –245.0 (s with satellites, J_{PtF} = 65.3 Hz). Elemental analysis calcd (%) for $C_{34}H_{33}FN_2Pt{\cdot}0.25CH_2Cl_2$: C 58.35, H 4.79, N 3.97; found: C 58.32, H 5.07, N 4.06.

[PtF(Ph)(thpy)$_2$] (6c). Pale yellow solid, obtained from **2c** (42 mg. 0.06 mmol) and AgF (15 mg, 0.14 mmol). Yield: 24 mg, 67%. ^{1}H NMR (400 MHz, CD_2Cl_2): δ 9.14 (d, J = 5.7 Hz, 1H), 7.92 (td, J = 7.9, 1.7 Hz, 1H), 7.72 (td, J = 7.8, 1.6 Hz, 1H), 7.59 (ddd, J = 8.0, 2.4, 1.2 Hz, 2H), 7.48 (d with satellites, J_{HH} = 5.1 Hz, J_{PtH} = 15.1 Hz, 1H), 7.48-7.37 (m, 2H), 7.32-7.16 (m, 2H), 6.97-6.86 (m, 6H), 6.31 (d, J_{HH} = 5.5 Hz, J_{PtH} = 19.3 Hz, 1H). ^{13}C{^{1}H} NMR (150.8 MHz, CD_2Cl_2): δ 158.7 (C), 158.3 (C), 147.0 (CH), 146.92 (CH), 141.1 (C), 140.8 (CH), 140.3 (CH),

135.7 (C), 134.1 (d, J_{CF} = 49.5 Hz, C), 133.7 (CH), 132.3 (J_{PtC} = 78.7 Hz, CH), 130.7 (J_{PtC} = 78.7 Hz, CH), 130.66, (CH), 129.58 (CH), 129.55 (CH), 128.7 (J_{PtC} = 72.2 Hz, CH), 127.5 (J_{PtC} = 48.4 Hz, CH), 126.4 (C), 125.1 (CH), 122.0 (CH), 121.8 (CH), 119.43 (CH), 119.39 (CH). ^{19}F NMR (282 MHz, CD_2Cl_2): δ –252.5 (s with satellites, J_{PtF} = 58.0 Hz). Elemental analysis calcd (%) for $C_{24}H_{17}FN_2PtS_2 \cdot 0.17CH_2Cl_2$: C 46.39, H 2.79, N 4.48, S 10.25; found: C 46.57, H 2.48, N 4.11, S 9.99.

[PtF(Ph)(piq)$_2$] (6d). White solid, obtained from **2d** (34 mg. 0.04 mmol) and AgF (10 mg, 0.08 mmol). Yield: 23 mg, 78%. ^{1}H NMR (400 MHz, CD_2Cl_2): δ 9.25 (dd with satellites, J_{HH} = 6.1, 1.2 Hz, J_{PtH} = 6.2 Hz, 1H), 9.02-8.95 (m, 1H), 8.93 (d, J_{HH} = 8.6 Hz, 1H), 8.30 (d, J = 8.0 Hz, 1H), 8.24 (d, J = 8.0 Hz, 1H), 8.04 (d, J = 8.0 Hz, 1H), 7.92 (d, J = 6.2 Hz, 1H), 7.86 (ddd, J = 8.1, 6.9, 1.2 Hz, 1H), 7.83-7.72 (m, 4H), 7.46-7.23 (m, 6H), 7.17 (ddd, J = 8.1, 6.9, 1.2 Hz, 1H), 6.97-6.77 (m, 6H). ^{13}C{^{1}H} NMR (150.8 MHz, CD_2Cl_2): δ 164.8 (J_{PtC} = 48.2 Hz, C), 162.8 (J_{PtC} = 53.4 Hz, C), 147.8 (J_{PtC} = 912.5 Hz, C), 144.7 (C), 143.0 (C), 139.13 (C), 139.07 (d, J_{CF} = 49.7 Hz, C), 138.6 (C), 138.1 (CH), 138.0 (CH), 137.98 (CH), 134.6 (J_{PtC} = 44.5 Hz, CH), 133.66 (J_{PtC} = 41.5 Hz, CH), 133.64 (CH), 133.1 (C), 133.0 (CH), 132.4 (CH), 132.24 (CH), 131.7 (CH), 131.6 (CH), 131.3 (J_{PtC} = 33.0 Hz, CH), 130.7 (J_{PtC} = 36.1 Hz, CH), 129.5 (CH), 129.2 (CH), 128.7 (CH), 128.1 (CH), 128.0 (CH), 127.6 (CH), 127.3 (CH), 126.9 (C), 126.8 (C), 125.0 (CH), 124.7 (CH), 124.6 (CH), 122.7 (CH). ^{19}F NMR (282 MHz, CD_2Cl_2): δ –238.8 (s with satellites, J_{PtF} = 85.4 Hz). Elemental analysis calcd (%) for $C_{36}H_{25}FN_2Pt$: C 61.80, H 3.60, N 4.00; found: C 61.85, H 3.56, N 4.10.

Conflicts of interest

There are no conflicts of interest to declare.

Acknowledgements

We thank Fundación Séneca (19890/GERM/15) and Ministerio de Ciencia, Innovación y Universidades (PGC2018-100719-BI00) for financial support. J.-C. López-López thanks Universidad de Murcia for a predoctoral fellowship.

References

1 K. K. W. Lo, *Acc. Chem. Res.*, 2015, **48**, 2985–2995.

2 A. M.-H. Yip and K. K.-W. Lo, *Coord. Chem. Rev.*, 2018, **361**, 138–163.

3 K. Y. Zhang, Q. Yu, H. Wei, S. Liu, Q. Zhao and W. Huang, *Chem. Rev.*, 2018, **118**, 1770–1839.

4 V. W. W. Yam, A. K. W. Chan and E. Y. H. Hong, *Nat. Rev. Chem.*, 2020, **4**, 528–541.

5 W.-P. To, Q. Wan, G. S. M. Tong and C.-M. Che, *Trends Chem.*, 2020, **2**, 796–812.

6 I. N. Mills, J. A. Porras and S. Bernhard, *Acc. Chem. Res.*, 2018, **51**, 352–364.

7 E. Longhi and L. De Cola, in *Iridium(III) in Optoelectronic and Photonics Applications*, John Wiley & Sons, Ltd, Chichester, UK, 2017, pp. 205–274.

8 Y. C. Wei, S. F. Wang, Y. Hu, L. S. Liao, D. G. Chen, K. H. Chang, C. W. Wang, S. H. Liu, W. H. Chan, J. L. Liao, W. Y. Hung, T. H. Wang, P. T. Chen, H. F. Hsu, Y. Chi and P. T. Chou, *Nat. Photonics*, 2020, **14**, 570–577.

9 T. Fleetham, G. Li and J. Li, *Adv. Mater.*, 2017, **29**, 1–16.

10 J. H. Shon and T. S. Teets, *Comments Inorg. Chem.*, 2020, **40**, 53–85.

11 D. M. Arias-Rotondo and J. K. McCusker, *Chem. Soc. Rev.*, 2016, **45**, 5803–5820.

12 W. P. To, T. Zou, R. W. Y. Sun and C. M. Che, *Philos. Trans. R. Soc. A Math. Phys. Eng. Sci.*, , DOI:10.1098/rsta.2012.0126.

13 D. L. Ma, H. Z. He, K. H. Leung, D. S. H. Chan and C. H. Leung, *Angew. Chem. Int. Ed.*, 2013, 52, 7666–7682.

14 F. Strieth-Kalthoff and F. Glorius, *Chem*, 2020, **6**, 1888–1903.

15 W. Lv, Y. Li, F. Li, X. Lan, Y. Zhang, L. Du, Q. Zhao, D. L. Phillips and W. Wang, *J. Am. Chem. Soc.*, 2019, **141**, 17482–17486.

16 F. Juliá, D. Bautista, J. M. Fernández-Hernández and P. González-Herrero, *Chem. Sci.*, 2014, **5**, 1875–1880.

17 F. Juliá, G. Aullón, D. Bautista and P. González-Herrero, *Chem. Eur. J.*, 2014, **20**, 17346–17359.

18 F. Juliá, D. Bautista and P. González-Herrero, *Chem. Commun.*, 2016, **52**, 1657–1660.

19 F. Juliá, M.-D. García-Legaz, D. Bautista and P. González-Herrero, *Inorg. Chem.*, 2016,

55, 7647–7660.

20 F. Juliá and P. González-Herrero, *Dalton Trans.*, 2016, **45**, 10599–10608.

21 N. Giménez, R. Lara, M. T. Moreno and E. Lalinde, *Chem. Eur. J.*, 2017, **23**, 5758–5771.

22 N. Giménez, E. Lalinde, R. Lara and M. T. Moreno, *Chem. Eur. J.*, 2019, **25**, 5514–5526.

23 Á. Vivancos, D. Bautista and P. González-Herrero, *Chem. Eur. J.*, 2019, **25**, 6014–6025.

24 Á. Vivancos, D. Poveda, A. Muñoz, J. Moreno, D. Bautista and P. González-Herrero, *Dalton Trans.*, 2019, **48**, 14367–14382.

25 J. C. López-López, D. Bautista and P. González-Herrero, *Chem. Eur. J.*, 2020, **26**, 11307–11315.

26 Á. Vivancos, A. Jiménez-García, D. Bautista and P. González-Herrero, *Inorg. Chem.*, 2021, **60**, 7900–7913.

27 C.-H. Lee, M.-C. Tang, F. K.-W. Kong, W.-L. Cheung, M. Ng, M.-Y. Chan and V. W.-W. Yam, *J. Am. Chem. Soc.*, 2020, **142**, 520–529.

28 M.-C. Tang, M.-Y. Leung, S.-L. Lai, M. Ng, M.-Y. Chan and V. Wing-Wah Yam, *J. Am. Chem. Soc.*, 2018, **140**, 13115–13124.

29 M.-C. Tang, C.-H. Lee, M. Ng, Y.-C. Wong, M.-Y. Chan and V. W.-W. Yam, *Angew. Chem. Int. Ed.*, 2018, **57**, 5463–5466.

30 R. Kumar and C. Nevado, *Angew. Chem. Int. Ed.*, 2017, **56**, 1994–2015.

31 W. P. To, D. Zhou, G. S. M. Tong, G. Cheng, C. Yang and C. M. Che, *Angew. Chem. Int. Ed.*, 2017, **56**, 14036–14041.

32 J. Fernandez-Cestau, B. Bertrand, A. Pintus and M. Bochmann, *Organometallics*, 2017, **36**, 3304–3312.

33 W. P. To, G. S. Tong, W. Lu, C. Ma, J. Liu, A. L. Chow and C. M. Che, *Angew. Chem. Int. Ed. Engl.*, 2012, **51**, 2654–2657.

34 P.-K. Chow, G. Cheng, G. S. M. Tong, C. Ma, W.-M. Kwok, W.-H. Ang, C. Y.-S. Chung, C. Yang, F. Wang and C.-M. Che, *Chem. Sci.*, 2016, **7**, 6083–6098.

35 P. K. Chow, C. Ma, W.-P. To, G. S. M. Tong, S.-L. Lai, S. C. F. Kui, W.-M. Kwok and C.-M. Che, *Angew. Chem. Int. Ed.*, 2013, **52**, 11775–11779.

36 J. Hu, M. Nikravesh, H. R. Shahsavari, R. Babadi Aghakhanpour, A. L. Rheingold, M. Alshami, Y. Sakamaki and H. Beyzavi, *Inorg. Chem.*, 2020, **59**, 16319–16327.

37 A. Maity, R. J. Stanek, B. L. Anderson, M. Zeller, A. D. Hunter, C. E. Moore, A. L. Rheingold and T. G. Gray, *Organometallics*, 2015, **34**, 109–120.

38 F. Juliá and P. González-Herrero, *J. Am. Chem. Soc.*, 2016, **138**, 5276–5282.

39 D. Poveda, Á. Vivancos, D. Bautista and P. González-Herrero, *Chem. Sci.*, 2020, **11**, 12095–12102.

40 L. Chassot, A. von Zelewsky, D. Sandrini, M. Maestri and V. Balzani, *J. Am. Chem. Soc.*, 1986, **108**, 6084–6085.

41 D. Sandrini, M. Maestri, V. Balzani, L. Chassot and A. Von Zelewsky, *J. Am. Chem. Soc.*, 1987, **109**, 7720–7724.

42 A. von Zelewsky, A. P. Suckling and H. Stoeckli-Evans, *Inorg. Chem.*, 1993, **32**, 4585–4593.

43 K. M. Altus, E. G. Bowes, D. D. Beattie and J. A. Love, *Organometallics*, 2019, **38**, 2273–2277.

44 R. H. Hill and R. J. Puddephatt, *J. Am. Chem. Soc.*, 1985, **107**, 1218–1225.

45 C. P. Andrieux and J. Pinson, *J. Am. Chem. Soc.*, 2003, **125**, 14801–14806.

46 A. J. Canty, J. Patel, T. Rodemann, J. H. Ryan, B. W. Skelton and A. H. White, *Organometallics*, 2004, **23**, 3466–3473.

47 N. J. Turro, V. Ramamurthy and J. C. Scaiano, *Principles of Molecular Photochemistry*, University Science Books, Sausalito, CA, 2009.

48 E. M. Kober, J. V Caspar, R. S. Lumpkin and T. J. Meyer, *J. Phys. Chem.*, 1986, **90**, 3722–3734.

49 G. S. Hill, M. J. Irwin, C. J. Levy, L. M. Rendina, R. J. Puddephatt, R. A. Andersen and L. McLean, in *Inorganic Syntheses*, ed. M. Y. Darensbourg, John Wiley & Sons, Inc., 1998, vol. 32, pp. 149–153.